TENSILE STRENGTH OF SURFACE NANOFIBERS IN TUNGSTEN

A.A. Mazilov[1], A.V. Noskov[2]
[1]National Science Center "Kharkov Institute of Physics and Technology", Kharkov, Ukraine;
[2]Belgorod State Technological University named after V.G. Shukhov, Belgorod, Russia
E-mail: alexey.mazilov@gmail.com

Recent studies carried out in linear plasma devices and tokamaks, have shown that low-energy He bombardment causes the creation of the nanofiber structure that leads to increased radiation erosion and material failure. One of the key characteristics of nanofibers is their mechanical strength. In this paper, a new mathematical technique was used for determination of the inherent tensile strength of nanofibers. The configuration of nanofibers was modeled by equipotential cylindrical surfaces. The potential distribution and mechanical stresses induced by high electric field were determined. An elaborated formalism was used to obtain the ultimate strength of tungsten nanofibers. The mean value of the tensile strength of tungsten nanofibers is equal to 27.52 GPa. This value is a substantial part of the theoretical tensile strength of tungsten.

PACS: 61.72.Mm, 62.40.+i, 61.66.-f

INTRODUCTION

Tungsten is the primary candidate for the divertors and blankets of next generation the fusion devices. Tungsten was chosen because of its high thermal conductivity and melting point, low sputtering erosion, and small tritium retention [1]. Earlier studies carried out in linear plasma apparatuses and tokamaks, have shown that low-energy He bombardment (in the region of 40…300 eV) causes the creation of nanoscale surface morphology known as 'fuzz' and formation of the nanofiber (nanotendril) structure [2] that leads to increased radiation erosion and material failure. The exact formation mechanism and mechanical properties of nanofiber structures remain indistinct.

The ultimate strength of metals realized in nanofibers is of great importance in the field of strong materials. Current advances in computing capabilities have made it achievable to use sophisticated atomic bonding potentials based on realistic theoretical considerations [3–5]. The ideal strength of a metal is a mechanical stress at which a perfect crystal becomes mechanically unstable and sets an upper limit of the material strength. The ultimate strength of materials is generally restricted by the nucleation and motion of dislocations and other lattice defects. For this reason, the strength, corresponding to the failure of a perfect, dislocation free metal, has hardly ever been achieved. The theoretical strength was nearly obtained in uniaxial tension experimental tests of whiskers [6], monoatomic chains [7] and nanoneedles [8]. The comparison of the ideal strength with the experimental measurements of strength of needle-shaped nanocrystals determined using the high-field field-ion microscopy (FIM) method [9] has shown that the ultimate strength is determined by heterogeneous nucleation of dislocations at the lateral surface of specimens. Modern nanoindentation researches showed that the yielding at the nanometer scale is controlled by homogeneous nucleation of dislocations under the indenter where the normal stresses approach the level near the theoretical strength of ideal crystals [10]. Nanosized objects have exceptionally high breaking stress, similar to that of ideal crystals and have prospective applications in anti-reflection coatings, scanning probe microscopy, and field ion and electron emission [11–13]. Theoretical analysis of the ultimate tensile strength of nanosized crystals comprises the computer simulation of phenomenological processes, such as plastic deformation at nanoscale level. However, the information on mechanical properties of such crystals at an atomic level is very limited. Experiments testing the ultimate strength of nanoobjects are very complicated, due to the difficulties in determination of the mechanical response of nanocrystals. Because of these difficulties, very little is known about mechanical properties of nanocrystals.

The normal stress acting near the surface of tip samples can be calculated if it is known the electric field at each point of the surface. Knowing the distribution of the normal to the surface component values of the stress tensor, it is possible to give an adequate description of the stress state of the whole sample. Although numerous attempts were made to solve this problem, at the present time it can be considered that it is completely solved only the task of determining of the stress field in the hemispherical part of the sample and calculations in general of the normal component of stress along the axis of the sample [14–17], that play an important role at the analytical definition of methods of field ion microscopy of needle nanocrystals strength on a breakaway.

The FIM has made it achievable to straightforwardly observe the atomic structure of nanocrystals under well-controlled crystallogeometric state combined with *in situ* mechanical loading in ultra-high electric fields. In these experiments, the nanocrystals subjected to high electric fields were fractured under tensile stresses close to the theoretical strength. An exceptional benefit of this method is the opportunity to avoid the intrinsic difficulty in nano-scale mechanical testings caused by the necessitate for assigning the cross-section area on which the tensile force is applied. The ultimate strength of nanocrystals at high-field testing could be determined by using only the field strength.

In this paper an analytical method for determination of the field strength on the top of the nanofibers was elaborated which is needed for accurate determination of the ultimate mechanical stresses for nanosized crystals in high electric fields. As a result, the upper limit of the tungsten strength has been determined.

1. ELECTROSTATIC APPROXIMATION OF NANOTIPS

To determine the tensile component of the normal stress σ_{zz} we define the configuration of the tip in cylindrical coordinates as $r = R(z)$. The tip is assumed axisymmetric and atomic-smooth. Find σ_{zz} in normal to axis of the sample cross-section by the plane $z = z_0$. The ponderomotive forces of the electric field lead to the appearance of tensile forces in the plane equal to

$$F_Z = \iint \frac{\varepsilon_0 E^2 \cos\alpha}{2} ds, \qquad (1)$$

where ds is the element of surface area, the normal to which makes an angle α with the z-axis. The integral is taken over the surface area of the sample from the vertex up to the plane $z = z_0$. Imagine ds as $2\pi r dl$ and, respectively:

$$F_Z = \int_0^{r_0} \frac{\varepsilon_0 E^2}{2} \frac{dr}{dl} 2\pi dl = \int_0^{r_0} \pi\varepsilon_0 E^2 dr, \qquad (2)$$

where $r_0 = R(z_0)$ is the radius-vector of the surface in the cross section by the plane $z = z_0$.

To determine the potential field in the vicinity of the tip sample surface it is proposed a number of models: parabolic, hyperbolic and "sphere-on-cone" [17, 18]. These approximations are not in all cases provide accurate descriptions of the real field emitters. The most flexible models, using only elementary functions [18], based on using of approximations of the surface configuration of the specimens by the equipotentials generated by charges distributions. Configuration of pulling electrodes, typically described by the same families of the equipotentials as a tip sample. At the same time, there are some peculiarities of the pulling electrodes geometry, that cannot be described within the framework of existing models. And presence of a circular aperture in pulling electrode is, mainly, of such features. However, the nature of the potential distribution at the sample surface, that determines the mechanical load on the sample, as estimates show, does not practically depend on the shape of pulling electrode (cathode). Taking into account these observations, the most convenient for solving problems related to the calculation of mechanical stresses, is a model, developed in [19].

In general case, the potential of the electric field, generated by uniformly charged semi-infinite wire, located along the negative axis z, with accuracy up to an arbitrary constant equal to:

$$\varphi(z,\rho,\theta) = \int_0^{\infty} \frac{\tau(\xi)d\xi}{4\pi\varepsilon_0\left[(z+\xi)^2+\rho^2\right]^{1/2}}, \qquad (3)$$

where ε_0 is an electric constant, equal $8.8542\cdot10^{-12}$ F/m, ξ is current coordinate along the charged wire, $\tau(\xi)$ is a linear charge density, satisfying the condition of finiteness of the field strength and specified by the equation:

$$\tau(\xi) = \tau + q\delta(\xi), \qquad (4)$$

where τ and q – constants that specify the magnitude of the charge on the wire top and a constant linear charge density, respectively. In dimensionless coordinates

$$\gamma=\rho/r_0 \text{ and } \eta=z/r_0, \qquad (5)$$

introducing parameter

$$\omega=q/\tau r_0, \qquad (6)$$

as a result of expression (3) integration, we obtain

$$\varphi(z,\rho,\theta) = \frac{V}{C_k - C_A}\left[C_k - \omega(\gamma^2+\eta^2)^{-1/2} + \ln\left(\sqrt{\gamma^2+\eta^2}+\eta\right)\right]. \qquad (7)$$

Here C_K and C_A – constants indicate the position of equipotentials, corresponding to the configuration of tip sample and pulling electrode, V is potential difference between sample and cathode. Equipotential that defines the shape of the tip surface is expressed by the ratio:

$$\omega\left(\gamma^2+\eta^2\right)^{-1/2} - \ln\left(\sqrt{\gamma^2+\eta^2}+\eta\right) = C_k, \qquad (8)$$

and configuration constants equal:

$$C_k = \omega - \ln 2 \text{ and } C_A = \frac{\omega}{\eta_{\max}} - \ln 2\eta_{\max}. \qquad (9)$$

The function $\eta = f(\gamma)$ describing the shape of the tip, in equation (8) taking into account (9) is set implicitly. There was written a special computer program for its determination. This program allows with defined precision to calculate and to display the shape of the tip surface with the given configuration parameter ω, and to calculate reduced field strength at any point on the surface.

Fig. 1 shows the equipotential lines corresponding to the configuration of the nanoobjects at different ratios of parameters of the electrostatic model.

Fig. 2 shows the dependence of the circles radii corresponding to the maximum and minimum of emitter cross-sections, from the configuration parameter of approximation ω.

2. FIELD STRENGTH CALCULATION

The local field strength can be obtained by differentiation of the expression (7):

$$F = \frac{V}{(C_K - C_A)r_0}\sqrt{\left[\omega\eta\left(\gamma^2+\eta^2\right)^{-3/2} + \left(\gamma^2+\eta^2\right)^{-1/2}\right]^2 + \left[\omega\gamma\left(\gamma^2+\eta^2\right)^{-3/2} + \frac{\gamma\left(\gamma^2+\eta^2\right)^{-1/2}}{\sqrt{\gamma^2+\eta^2}+\eta}\right]^2}. \qquad (10)$$

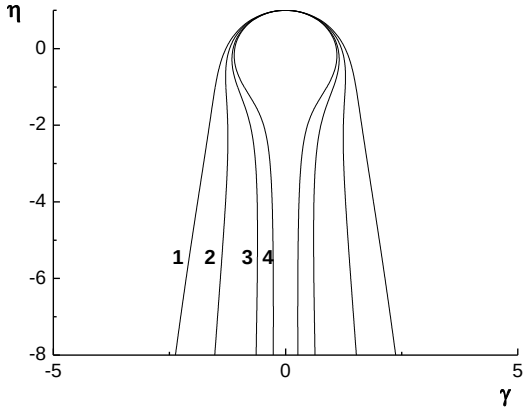

Fig. 1. Approximation of configuration of the nanoobjects by equipotentials that are generated by uniformly charged semi-infinite wire with additional point charge at its beginning:
1 – ω=2; 2 – ω=3; 3 – ω=5; 4 – ω=7

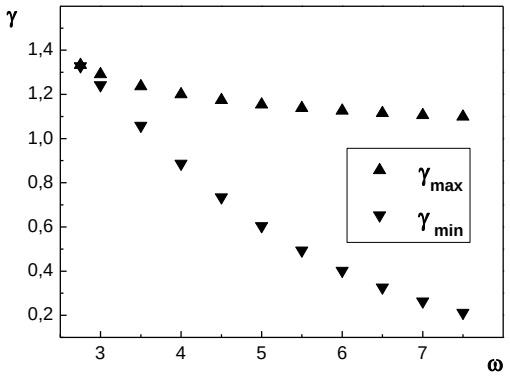

Fig. 2. The dependence of reduced circles radii corresponding to the maximum and minimum of nanoobjects cross-sections, from the approximation parameter ω

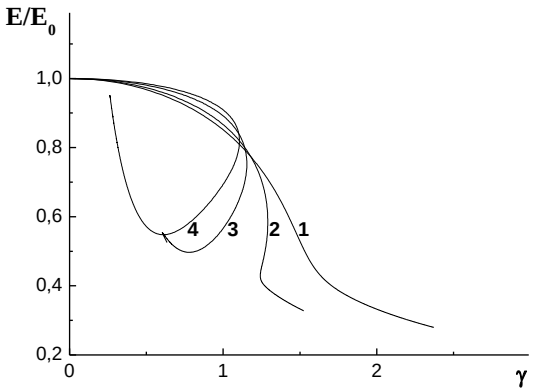

Fig. 3. The dependence of reduced field strength from the dimensionless radial coordinate for nanoobjects of different configurations, calculated from equation (10):
1 – ω = 2; 2 – ω = 3; 3 – ω = 5; 4 – ω = 7

The field strength at the top of the emitter can be represented as:

$$F_0 = \frac{V(\omega+1)}{r_0\left[(\omega-\ln 2)+\ln 2\eta_{\max}\right]}. \qquad (11)$$

For a parabolic tip, as is known, the relation is valid [17, 20]

$$F_0 \cong \frac{2V}{r_0 \ln\left(2R_0 / r_0\right)}. \qquad (12)$$

Comparing equations (11) and (12) when the approximation parameter $\omega = 2$, corresponding parabolic configuration of the tip, we can see that the results of the field strength calculations for these equations are similar. That indicates applicability of the approximation.

Fig. 3 shows graphs of dependence of reduced local field strength from dimensionless coordinate γ. The complex nature of the dependence when $\omega > 3$ is explained by the ambiguity of the function $E(\gamma)$ for samples with a thickening at the top.

3. MECHANICAL STRESSES CALCULATION

It is known that mechanical stresses play a decisive role in the destruction of samples in process of their forming by field evaporation. Mechanical tensile stresses along the axis of the emitters defined by the relation (2) for complex configurations can be represented in form of two integrals

$$\langle\sigma_{zz}\rangle = \frac{\varepsilon_0}{\gamma_{\min}}\left[\int_0^{\gamma_{\max}} F^2(\gamma)\gamma d\gamma - \int_{\gamma_{\min}}^{\gamma_{\max}} F^2(\gamma)\gamma d\gamma\right]. \qquad (13)$$

Here the first integral describes the stretching of the emitter by the electric field, and the second one – his pressure on the surface area with negative normal.

The maximum value mechanical tensile stresses along the axis of the emitter for different configurations specified by approximation parameter ω (Fig. 4), was calculated by integration of the expression (1) taking into account changes in the local field strength (10).

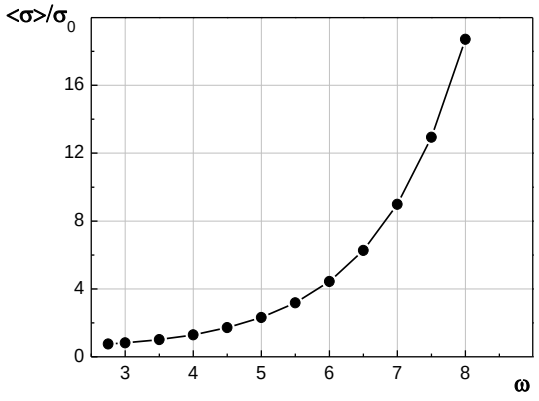

Fig. 4. Reduced maximum values of tensile stress for different configurations of emitters specified by approximation parameter ω

The calculations were performed according to the formula

$$\frac{\langle\sigma_{zz}\rangle}{\sigma_{zz}(0)} = \frac{2}{\gamma_{\min}^2}\left[\int_0^{\gamma_{\max}} \frac{F^2(\gamma)}{F_0^2}\gamma d\gamma - \int_{\gamma_{\min}}^{\gamma_{\max}} \frac{F^2(\gamma)}{F_0^2}\gamma d\gamma\right]. \qquad (14)$$

Fig. 5 presents reduced maximum values of mechanical tensile stresses in the emitter for different radii of the head and neck at the top of the sample. The

results obtained are satisfactorily approximated by a parabolic equation

$$\langle\sigma\rangle/\sigma_0 = \alpha\left(\gamma_{\max}/\gamma_{\min}\right)^{\beta}, \qquad (15)$$

where $\alpha = 0.71$, $\beta = 1.69$. This expression agrees satisfactorily with the semi-empirical correlation for determination of the density of ponderomotive forces on the emitter surface with a thickening at apex, obtained earlier in [20–23]. This difference may be due to the fact that in [20, 22] was used qualitatively different scheme of the potential distribution approximation.

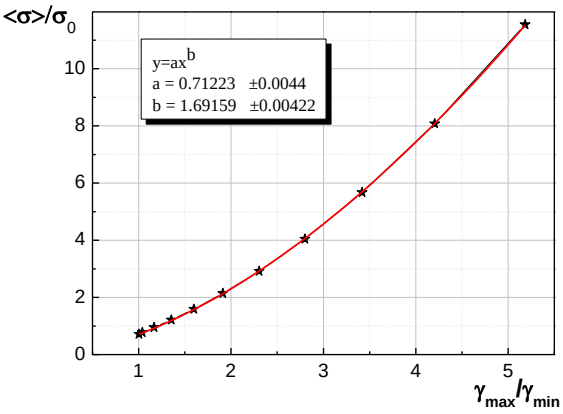

Fig. 5. The dependence of reduced maximum values of mechanical tensile stresses in the emitter from the relationship of the radii of the head and neck

The obtained equation (15) can be used to give a more precise value for ultimate strength of nanocrystals which corresponds to a nearly theoretical level of strength. As was shown in [22], the failure of FIM specimens triggered by the electrical forces has a statistical character. It was pointed out that the detached specimen fragments might possess a configuration far from spherical with low accuracy for determination of configuration. To avoid this technical problem, a special configuration of FIM specimens was used in experiments on a high-field failure [22]. The radius of the thickened spherical cap R and the neck parts r of the specimens were determined from transmission electron micrographs. The samples were loaded by the mechanical stress produced by electric fields. The uniaxis tensile strength was taken to be the maximum stress withstood by a specimen before fracture. Specimen failure was determined by the appearance of characteristic field-ion microfractograms and was usually observed to be correlated with a light flash in the interelectrode space of the FIM. The voltage V applied to the gap was increased gradually until a breakdown phenomenon occurred. As can be shown from Eqs. (2) and (15), for samples with the ratio R/r the breaking stress is given by

$$\sigma = \frac{\alpha\varepsilon_0 E^2}{2}\left(\frac{R}{r}\right)^{\beta}, \qquad (16)$$

where E is the field strength at the apex of specimen, α is a numerical coefficient equal to 0.71 for samples with thermally smoothed surface, and $\beta = 1.69$ as in Eq. (15). The deviation of β from two is due to the presence of compressive components of the stress near the necks of samples. For determination of tensile strength, we used experimental data obtained on the field ion specimens of particular configurations. Such specimens with neck constriction were obtained [21] by heating nanofibers (nanotendrils) at 1400…1600 °C for 10…15 min. The radius of the spherical cap R and the neck regions r (Fig. 6) were determined from electron micrographs. The samples were loaded by the mechanical stress produced by electric fields. Specimen breakage was determined by field-ion microfractograms.

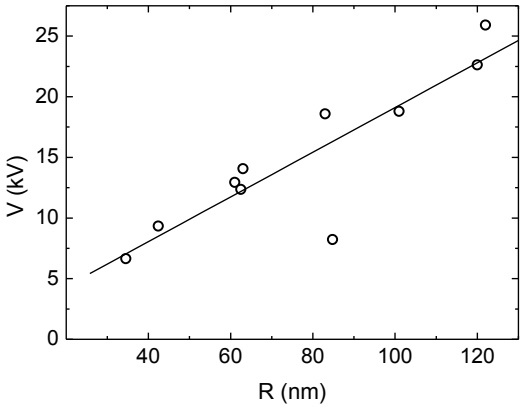

Fig. 6. Dependence of breakdown voltages on the radius of the tip

The field value at the apex of the tip is given by [13]

$$E = \frac{V}{k_f R}, \qquad (17)$$

where k_f is the geometric field coefficient, which slightly depends on the taper angle of the specimen. An average voltage of the tip failure is equal to

$$V_f = k_f R\left[\frac{2\sigma_f}{\alpha\varepsilon_0}\left(\frac{r}{R}\right)^{\beta}\right]^{1/2}, \qquad (18)$$

where σ_f is the mean value of the tensile strength of the specimens. Using the experimental data on r, R, and V_f from [21] shown in Fig. 6 it was obtained the mean value of the tensile strength of tungsten nanofibers equal to 27.52 GPa. This value is about 30% below the theoretical tensile strength of tungsten [24]. This comparison allowed to arrive at the suggestion that observed lowering of the strength can be caused by nucleation of dislocations at the free specimen surface.

CONCLUSIONS

1. A new mathematical technique was used for determination of the inherent tensile strength of nanofibers usually produced in linear plasma apparatuses and tokamaks under low-energy He bombardment.

2. Analytical expression for determination of the field strength on the top of the nanocrystals of different configurations was found out. It was established that under small values of the configuration parameter, equipotentials get form, close to parabolic. Under these conditions, the obtained expression is transformed into a

well-known relation for parabolic tips used in electronics emission and corpuscular optics. This demonstrates the applicability of used approximation to describe the potential distribution near the surface of the nanotips.

3. It was calculated potential distribution, field strength and induced by electric field stress at the surface of nanofibers of complex configuration that cannot be described mathematically by quadric surfaces. Thereby it was created an analytical basis for calculation of electron and ion optics for field emission microscopy of nanoobjects.

4. An elaborated formalism was used to obtain the ultimate strength of tungsten nanofibers. The mean value of the tensile strength of tungsten nanofibers is equal to 27.52 GPa. This value is a substantial part of the theoretical tensile strength of tungsten.

ACKNOWLEDGEMENTS

We are very obliged to V.A. Ksenofontov and I.M. Mikhailovskij for useful discussions and comments.

REFERENCES

1. G. Janeschitz. ITER JCT and HTs. Plasma – wall interaction issues in ITER // *Journal of Nuclear Materials*. 2001, v. 290, p. 1-11.

2. M.J. Baldwin, T.C. Lynch, R.P. Doerner, and J.H. Yu. Nanostructure formation on tungsten exposed to low-pressure rf helium plasmas: a study of ion energy threshold and early stage growth // *Journal of Nuclear Materials.* 2011, v. 415, p. S104-S107.

3. W. Luo, D. Roundy, M.L. Cohen, and J.W. Morris. Ideal strength of bcc molybdenum and niobium // *Physical Review*. 2002, v. B66, p. 094110.

4. M. Černý, M. Šob, J. Pokluda, and P. Sandera. *Ab initio* calculations of ideal tensile strength and mechanical stability in copper // *Journal of Physics: Condensed Matter*. 2004, v. 16, p. 1045.

5. M. Šob, J. Pokluda, M. Černý, P. Šandera, and V. Vitek. Theoretical Strength of Metals and Intermetallics from First Principles // *Materials Science Forum. Materials Structure & Micromechanics of Fracture*. 2005, v. 482, p. 33.

6. A. Kelly and N.H. Macmillan. *Strong Solids*, Clarendon, Oxford and references therein, 1986.

7. S. Kotrechko, I. Mikhailovskij, T. Mazilova, E. Sadanov, A. Timoshevskii, N. Stetsenko, Y. Matviychuk. Mechanical properties of carbyne: experiment and simulations // *Nanoscale Research Letters*. 2015, v. 10(1), p. 24.

8. A.P. Shpak, S.O. Kotrechko, T.I. Mazilova, I.M. Mikhailovskij. Inherent tensile strength of molybdenum nanocrystals // *Science and Technology of Advanced Materials*. 2009, v. 10, p. 045004.

9. A. Bakai, A. Shpak, N. Wanderka, S. Kotrechko, T. Mazilova, & I. Mikhailovskij. Inherent strength of zirconium-based bulk metallic glass // *Journal of Non-Crystalline Solids*. 2010, v. 356(25-27), p. 1310-1314.

10. J.R. Greer and W.D. Nix. Size dependence of mechanical properties of gold at the sub-micron scale // *Applied Physics.* 2005, v. A80, p. 1625.

11. Y.M. Wang and E. Ma. On the origin of ultrahigh cryogenic strength of nanocrystalline metals // *Applied Physics Letters.* 2004, v. 85, p. 2750.

12. S. Chattopadhyay, L.-C. Chen, and K.-H. Chen. Nanotips: Growth, Model, and Applications // *Critical Review in Solid State and Materials Sciences*. 2006, v. 31, p. 15.

13. T.I. Mazilova, I.M. Mikhailovskij. Atomic mechanism of radiation-induced erosion of field electron emitters // *Surface and Interface Analysis*. 2004, v. 36(5-6), p. 510-514.

14. V.A. Ksenofontov, T.I. Mazilova, E.V. Sadanov, I.M. Mikhailovskij, O.A. Velicodnaja, A.A. Mazilov. High-field formation and field ion microscopy of monatomic carbon chains. // *Journal of Physics: Condensed Matter*. 2007, v. 19(46), p. 466204.

15. T.T. Tsong. Atom-probe and field ion microscopy: Field ion emission and surfaces and interfaces at atomic resolution // *Cambridge University Press*. Cambridge, 1990, 387 p.

16. M.K. Miller, A. Cerezo, M.G. Heatherington, and G.D.W. Smith. *Atom probe field ion microscopy*. Clarendon, Oxford, 1996, 509 p.

17. R. Gomer. *Field emission and field ionization, Harvard Univ.* Press, Cambridge, 1961, 195 p.

18. П.А. Березняк, В.В. Слезов. *Радиотехника и электроника*. 1972, т. 2, с. 354.

19. D.J. Rose. On the Magnification and Resolution of the Field Emission Electron Microscope // *Journal of Applied Physics.* 1956, v. 27, v. 3, p. 215.

20. I.M. Mikhailovskij, P.Ya. Poltinin, L.I. Fedorova // *Sov. Phys. Solid State*. 1981, v. 23, p. 757.

21. V.A. Ksenofontov. A structure at the atomic level of nanosized and nanostructure metallic and carbon materials: *Thesis for D. Sc. Degree in physics and mathematics.* Kharkiv, 2011.

22. I.M. Mikhailovskij, N. Wanderka, V.E. Storizhko, V.A. Ksenofontov, T.I. Mazilova. A new approach for explanation of specimen rupture under high electric field // *Ultramicroscopy*. 2009, v. 109, p. 480-485.

23. A.A. Mazilov. Determination of the spectra of ion He and H_2 bombardment of autoemitter surface // *Problems of Atomic Science and Technology. Series "Physics of Radiation Effects and Radiation Materials Science"*. 2015, №2 (96), p. 35-38.

24. D. Roundy, C.R. Krenn, M.L. Cohen, J.W. Morris. The ideal strength of tungsten // *Jr. Philosophical Magazine*. 2001, v. A81, p. 1725-1747.

Article received 14.02.2019

ПРОЧНОСТЬ НА РАСТЯЖЕНИЕ ПОВЕРХНОСТНЫХ ВОЛЬФРАМОВЫХ НАНОФИБРИЛЛ

А.А. Мазилов, А.В. Носков

Недавние исследования, проведенные на линейных плазменных устройствах и токамаках, показали, что низкоэнергетическая бомбардировка атомами Не вызывает создание структуры из нанофибрилл, что приводит к усилению радиационной эрозии и разрушению материала. Одной из ключевых характеристик нанофибрилл является их механическая прочность. В этой статье был использован новый математический метод для определения собственной прочности нанофибрилл на растяжение. Конфигурация нанофибрилл моделировалась эквипотенциальными цилиндрическими поверхностями. Определены распределение потенциала и механические напряжения, вызванные сильным электрическим полем. Разработанный формализм был использован для получения предельной прочности вольфрамовых нанофибрилл. Среднее значение прочности на разрыв вольфрамовых нанофибрилл равно 27,52 ГПа. Эта величина является существенной частью теоретической прочности на растяжение вольфрама.

МІЦНІСТЬ НА РОЗТЯГУВАННЯ ПОВЕРХНЕВИХ ВОЛЬФРАМОВИХ НАНОФІБРІЛ

О.О. Мазілов, А.В. Носков

Недавні дослідження, проведені на лінійних плазмових пристроях і токамаках, показали, що низькоенергетичне бомбардування атомами Не викликає створення структури з нанофібріл, що призводить до посилення радіаційної ерозії і руйнування матеріалу. Однією з ключових характеристик нанофібріл є їх механічна міцність. У цій статті був використаний новий математичний метод для визначення власної міцності нанофібріл на розтягнення. Конфігурація нанофібріл моделювалася еквіпотенціальними циліндричними поверхнями. Визначено розподіл потенціалу та механічні напруги, викликані сильним електричним полем. Розроблений формалізм був використаний для отримання граничної міцності вольфрамових нанофібріл. Середнє значення міцності на розрив вольфрамових нанофібріл дорівнює 27,52 ГПа. Ця величина є суттєвою частиною теоретичної міцності на розтягнення вольфраму.